



Scholastic modeling of pH and redox potential changes in olive tree leaf alcohol and acids containing incubation media designed for the steady growth of *Acetobacter aceti* and *Saccharomyces cerevisiae*

Yakup Ermurat 

Bolu Abant Izzet Baysal University, Department of Chemical Engineering, Engineering Faculty, Bolu, Turkiye

ARTICLE INFO

Research Article

Article History:

Received: 6 April 2023

Accepted: 24 July 2023

Available Online: 26 July 2023

Keywords:

Steady growth of *Acetobacter aceti* and*Saccharomyces cerevisiae*,

Olive tree leaf powder

Effects of acids and alcohol

pH and redox potential modeling

Field Emission Gun – Scanning Electron

Microscope (FEG-SEM)

ABSTRACT

Modeling of pH and redox potential changes was investigated instructionally in incubation media designed for a stable growth of *Acetobacter aceti* and *Saccharomyces cerevisiae*. Olive tree leaf, phosphoric acid, vinegar, acetic acid and ethyl alcohol were used in incubation for extraction and symbiotic purposes. Structure imaging of olive tree leaf powder was performed using the Field Emission Gun – Scanning Electron Microscope (FEG-SEM). The incubation experiments were carried out at initially lowest pH and high temperatures of 30 °C and 35 °C for eight days in liquid state fermentation process. A steady *A. aceti* and *S. cerevisiae* growth was observed during the incubation. Increase in pH value displayed increase in redox potential in water+ phosphoric acid, vinegar+A. *aceti*+phosphoric acid, *S. cerevisiae*+A. *aceti*+acetic acid+phosphoric acid and *S. cerevisiae*+A. *aceti*+phosphoric acid solution processes at 30 °C, and acetic acid+phosphoric acid and vinegar+phosphoric acid solution processes at 35 °C. Decrease in pH value displayed decrease in redox potential in A. *aceti*+alcohol+phosphoric acid, vinegar+phosphoric acid, *S. cerevisiae*+A. *aceti*+acetic acid+phosphoric acid and *S. cerevisiae*+A. *aceti*+phosphoric acid solution processes at 30 °C, and vinegar+A. *aceti*+phosphoric acid, *S. cerevisiae*+A. *aceti*+acetic acid+phosphoric acid and *S. cerevisiae*+A. *aceti*+phosphoric acid solution processes at 35 °C.

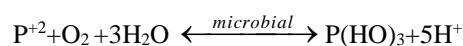
1. Introduction

Investigation of educational modeling of chemical, biochemical and biological parameters of an incubation media is assumed to be a fundamental way to understand the steady growth essentials of organisms in a lowest pH liquid media at a high growth temperature. Study of the impact of chemicals and biochemicals such as alcohol, vinegar, acetic acid, phosphoric acid and phenolic components of olive leaf on growth of organisms such as *Acetobacter aceti* and *Saccharomyces cerevisiae* is significant to determine the effects of the growth essentials (Ermurat 2013; Borjan et al., 2020; Qabaha et al., 2018).

Extraction of phenolic components from the olive leaf is dependent on the alcohol and acids which affect pH and redox potential in the incubation media. Decrease in pH and redox potential would have an increasing effect on dissolution of bioactive compounds such as phenolic substances stored in the olive leaf. The main component of the phenolic substances is oleuropein, a glucoside polysaccharide which has approved medicinal potential as antioxidant. Studies have stated that the olive leaf has higher bioactivity compared to other various olive

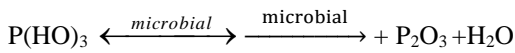
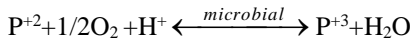
products (Topuz & Bayram 2021; Markhali et al., 2020).

Therefore, the effects of, phenolic substances, ethyl alcohol (C₂H₅OH), inorganic acids such as phosphoric acid (H₃PO₄), and organic acids like acetic acid (CH₃COOH) were studied to understand the implication of these biochemicals and chemicals on the stable growth of microorganisms. The bioprocesses of microorganisms in liquid media can be assessed by monitoring the changes in the pH and redox potential values. When the pH value decreases, the activity of microorganisms weakens, but production of metabolites by microorganisms increases (Chen et al., 2022; Radak et al., 2017). At low pH values, phosphate ions are predominantly present, and the high concentration of PO₄⁻ is a major factor responsible for the high phosphorylation rates. The chemical effect of phosphoric acid on the growth of living cells plays a significant role for phosphorylation processes. The bioprocess of phosphorylation involves a primary acidic or oxidative phosphor reaction process. The oxidation of phosphorylation process through microorganisms consists of subsequent reactions. It has estimated that phosphor ions are generated through microbial oxidation with oxygen:

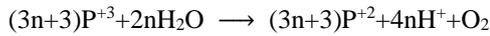


*Corresponding author

E-mail address: yakupermurat@ibu.edu.tr



The simplified stoichiometry of the bio-chemical phosphor oxidation process can be written as:



The key role of the microorganisms in phosphorylation process is to regenerate the phosphor ion and maintain a sufficiently high redox potential for the reaction to proceed and to oxidize the phosphor product and maintain a low pH, which means protons consumed, by the phosphorylation reactions to supply phosphor ions. The biomolecular structures of the free nucleotides, one of the vital phosphate mineral residues, form phosphodiester bonds by attaching to pentose sugar molecules at the 3' carbon and 5' C positions. The bases of genetic molecules are attached to the 1' carbon of the pentose residues, and adenosine three phosphates (ATP) form a covalent bond between phosphate and amino acid in the enzyme that may have a charge and affects the chemistry of the reactants (Tarrant & Cole, 2009; Neuer et al., 1983).

Acetic acid bacteria (AAB), well known as the nutrition grade vinegar producing bacteria, are obligate aerobes that able to oxidize ethanol and sugars into acetic acid. The optimal temperature for growth is between 25 to 30 °C, and the pH optimum between 5.4 and 6.3. The members of the genus AAB is traditionally and industrially used for production of vinegar acetic acid and grows well with ethanol as a source of carbon, however glucose has been shown to actually decrease the growth rate in culture, especially when other carbon sources were present (Ory et al., 1998; O'Sullivan & Ettlinger, 1976). Symbiotic work between *Saccharomyces* and *Acetobacter* yields glucose conversion to alcohol ending acetic acids (Krisch & Szajani 1997; Krisch & Szajáni 1996).

The relationship between pH and redox potential is based on the proton concentration, which directly affects the electron exchanges in aqueous solutions. This study was planned to investigate the modeling of the active effects of pH and redox potential changes on constant growth of *A. aceti* and *S. cerevisiae* incubated in olive leaf, phosphoric acid, ethyl alcohol, vinegar and acetic acid containing media at high growth temperature.

2. Materials and Methods

The wet olive leaf was provided directly from the trees in central Kahramanmaraş region, dried away from the exposure of sun light at room temperature and roughly grinded to powder form by hand without using any grinding equipment. The powder sample of pure dry olive tree leaf was used for very highest resolution microstructural imaging using the Field Emission Gun – Scanning Electron Microscope (FEG-SEM). The preparation of the mixture of the incubation media material was formulated as 1% quantity of olive tree leaf powder pulp and 0.1% phosphoric acid, acetic acid, vinegar and ethyl alcohol solutions each. The wild strains of *A. aceti* were isolated from vinegar solutions through the incubation at 30 °C on glucose-yeast extract-calcium carbonate (GYC) medium. *S. cerevisiae* strains were supplied from commercial yeast. Approximated numbers of *A. aceti* and *S. cerevisiae* strains were initiated as 1×10^5 cells per mL. Different combinations

of incubation media solutions were prepared using *A. aceti*, *S. cerevisiae*, olive leaf powder, phosphoric acid, ethyl alcohol, vinegar and acetic acid. pH and mV measurements were carried out by using Hanna instruments. The pH value was not buffered at a steady state value through the incubation experiments that were carried out at high fixed growth temperatures of 30 °C and 35 °C for eight days.

3. Results

The experimental observations of pH and mV versus time were graphed to investigate the effect of low pH and redox potential changes on microbial growth of *A. aceti* and *S. cerevisiae* incubated in olive leaf powder, phosphoric acid, ethyl alcohol, vinegar and acetic acid containing media combinations at the fixed high growth temperatures.

The graphs of pH and mV versus time were given in Figures 1-16 showing the polynomial equations and R^2 values at the high growth temperatures of (◆) 30 °C and (■) 35 °C.

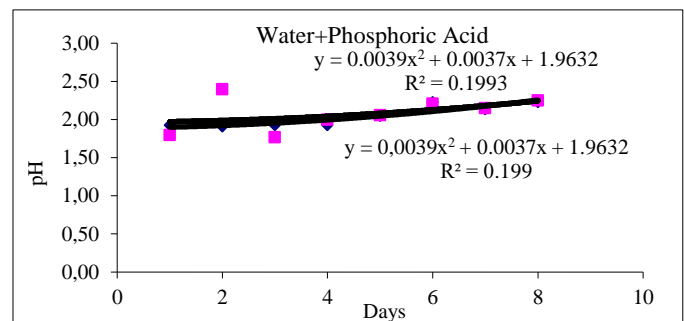


Figure 1. pH changes for water + phosphoric acid

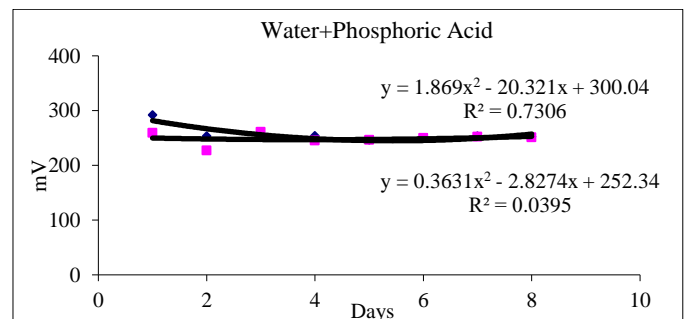


Figure 2. mV changes for water + phosphoric acid mixture

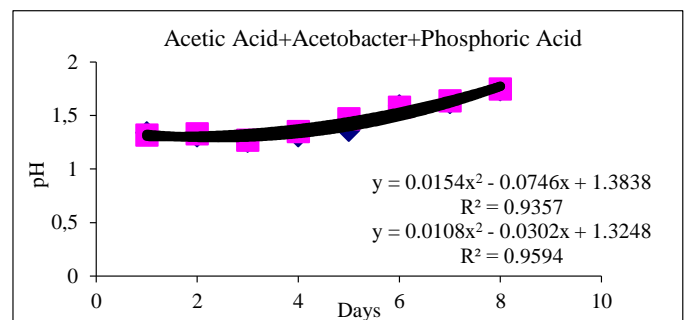


Figure 3. pH changes for acetic acid + *A. aceti* + phosphoric acid mixture

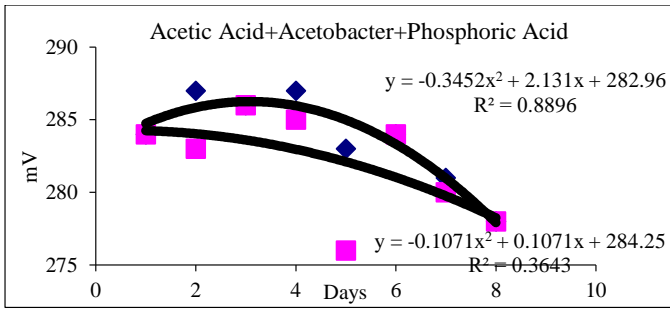


Figure 4. mV changes for acetic acid + *A. aceti* + phosphoric acid mixture

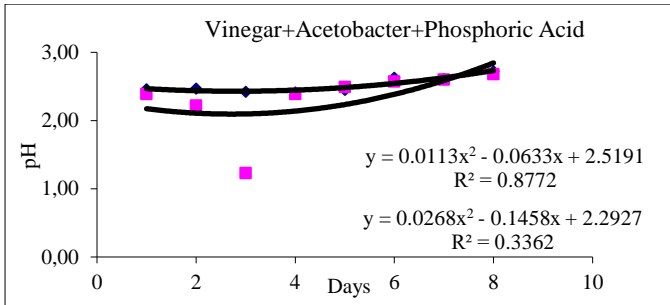


Figure 5. pH changes for vinegar + *A. aceti* + phosphoric acid mixture

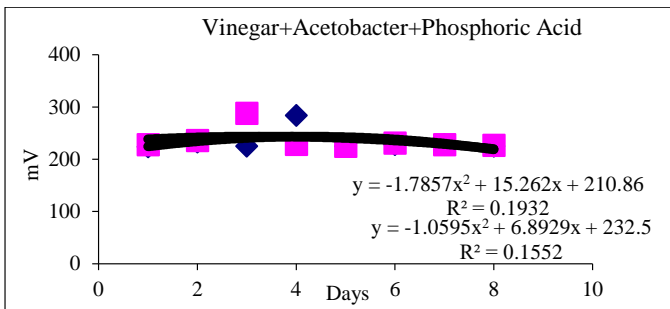


Figure 6. mV changes for vinegar + *A. aceti* + phosphoric acid mixture

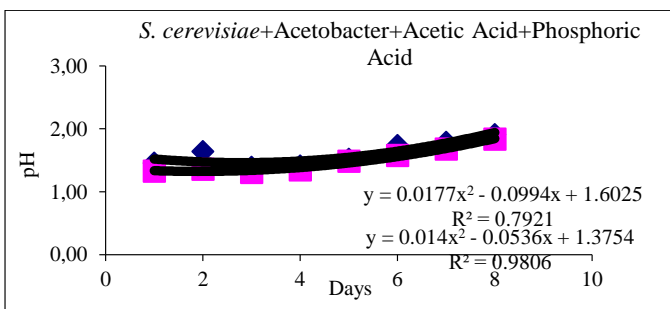


Figure 7. pH changes for *S. cerevisiae* + *A. aceti* + acetic acid + phosphoric acid mixture

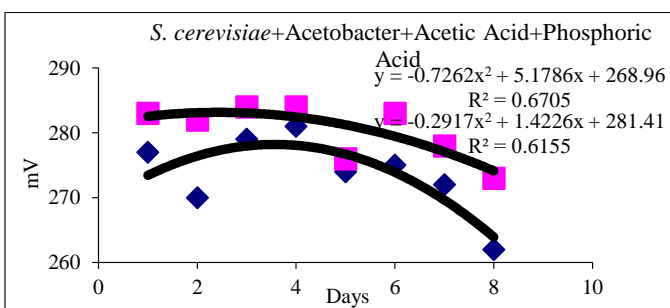


Figure 8. mV changes for *S. cerevisiae* + *A. aceti* + acetic acid + phosphoric acid mixture

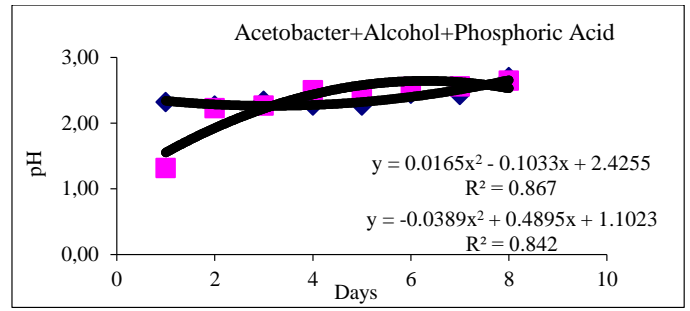


Figure 9. pH changes for *A. aceti* + Alcohol + phosphoric acid mixture

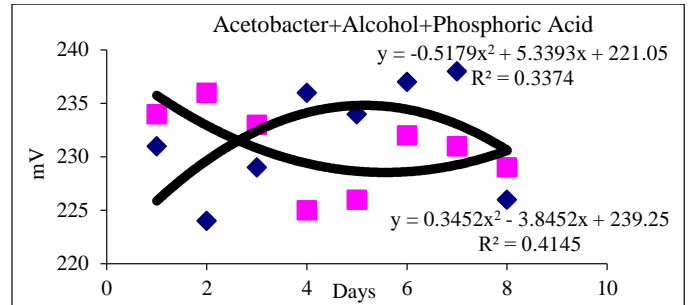


Figure 10. mV changes for *A. aceti* + Alcohol + phosphoric acid mixture

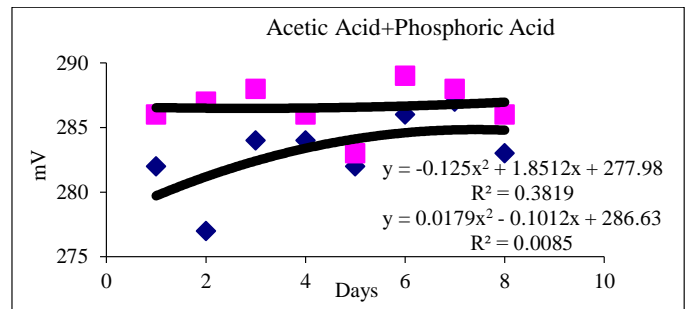


Figure 11. pH changes for acetic acid + phosphoric acid mixture

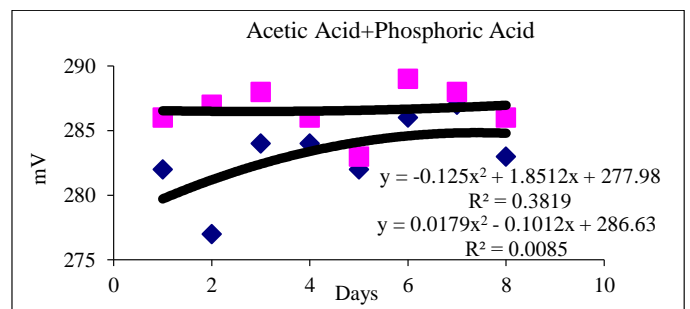


Figure 12. mV changes for acetic acid + phosphoric acid mixture

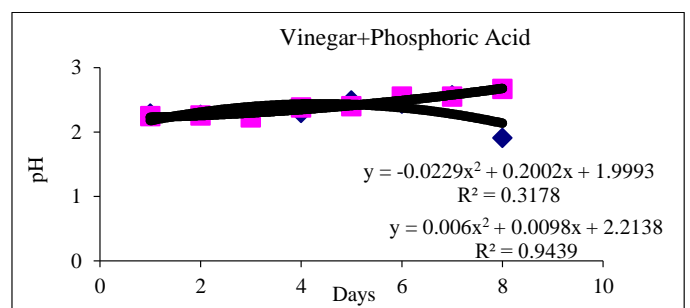


Figure 13. pH changes for vinegar + phosphoric acid mixture

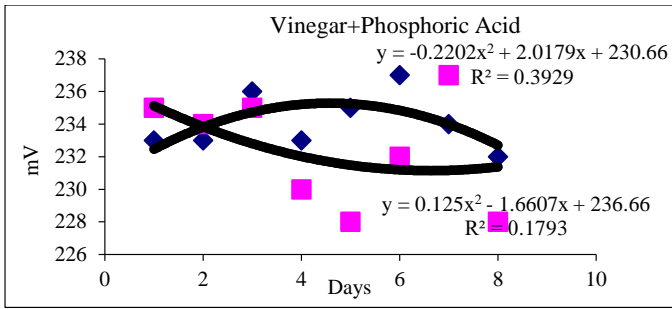


Figure 14. mV changes for vinegar + phosphoric acid mixture

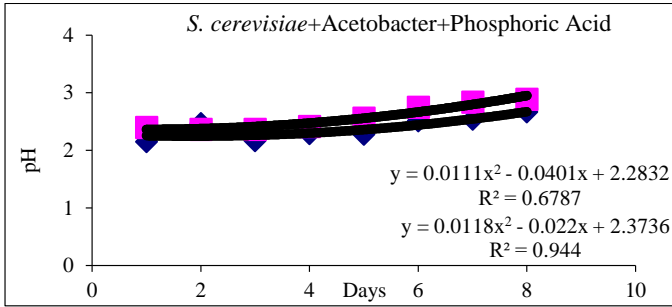


Figure 15. pH changes for *S. cerevisiae* + *A. aceti* + phosphoric acid mixture

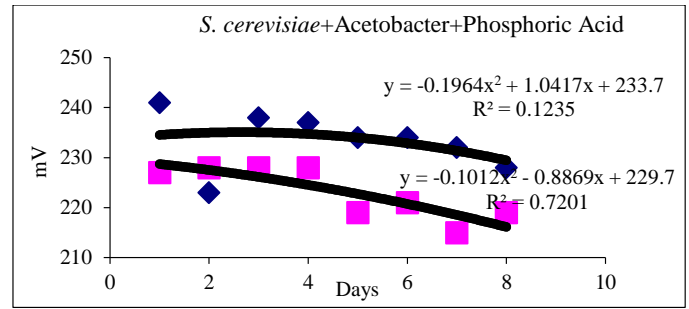


Figure 16. mV changes for *S. cerevisiae* + *A. aceti* + phosphoric acid mixture

Table 1 shows the extracted polynomial equations, R^2 values and their first derivatives in linearized forms.

The derivative equations were used to get predictive pH and mV values and draw kinetic velocity graphs as shown through Figures 17 to 32.

Table 1. Polynomial equations, R^2 values and their first derivatives

Pulp solutions		T°C	Polynomial equation	R^2	First derivatives
Water + phosphoric acid	pH=y	30	$y=0.0039x^2+0.0037x+1.9632$	0.1993	$dy/dx=0.0078x+0.0037$
	t=x	35	$y=0.0039x^2+0.0037x+1.9632$	0.1993	$dy/dx=0.0078x+0.0037$
	mV=y	30	$y=1.869x^2-20.321x+300.04$	0.7306	$dy/dx=3.738x-20.321$
	t=x	35	$y=0.3631x^2-2.8274x+252.34$	0.0395	$dy/dx=0.7262x-2.8274$
Acetic acid + <i>A. aceti</i> + phosphoric acid	pH=y	30	$y=0.0154x^2-0.0746x+1.3838$	0.9357	$dy/dx=0.0308x-0.0746$
	t=x	35	$y=0.0108x^2+0.00302x+1.3248$	0.9594	$dy/dx=0.0216x+0.00302$
	mV=y	30	$y=-0.3452x^2+2.131x+282.96$	0.8896	$dy/dx=-0.6904x+2.131$
	t=x	35	$y=-0.1071x^2+0.1071x+284.25$	0.3643	$dy/dx=-0.2142x+0.1071$
Vinegar + <i>A. aceti</i> + phosphoric acid	pH=y	30	$y=0.0113x^2-0.0633x+2.5191$	0.8772	$dy/dx=0.0226x-0.0633$
	t=x	35	$y=0.0268x^2+0.1458x+2.2927$	0.3362	$dy/dx=0.0536x+0.1458$
	mV=y	30	$y=-1.7857x^2+15.262x+210.86$	0.1932	$dy/dx=-3.5714x+15.262$
	t=x	35	$y=-1.0595x^2+6.8929x+232.5$	0.1552	$dy/dx=-2.119x+6.8929$
<i>S. cerevisiae</i> + <i>A. aceti</i> + acetic acid + phosphoric acid	pH=y	30	$y=0.0177x^2-0.0994x+1.6025$	0.7921	$dy/dx=0.0354x-0.0994$
	t=x	35	$y=0.014x^2-0.0536x+1.3754$	0.9806	$dy/dx=0.028x-0.0536$
	mV=y	30	$y=-0.7262x^2+5.1786x+268.96$	0.6705	$dy/dx=1.4524x+5.1786$
	t=x	35	$y=-0.2917x^2+1.4226x+281.41$	0.6155	$dy/dx=-0.5834x+1.4226$
<i>A. aceti</i> + alcohol + phosphoric acid	pH=y	30	$y=0.0165x^2-0.1033x+2.4255$	0.867	$dy/dx=-0.033x-0.1033$
	t=x	35	$y=-0.0389x^2+0.4895x+1.1023$	0.842	$dy/dx=-0.0778x+0.4895$
	mV=y	30	$y=-0.5179x^2+5.3393x+221.05$	0.3374	$dy/dx=-1.0358x+5.3393$
	t=x	35	$y=0.3452x^2-3.8452x+239.25$	0.4145	$dy/dx=0.6904x-3.8452$
Acetic acid + phosphoric acid	pH=y	30	$y=0.0121x^2-0.0712x+1.4538$	0.8302	$dy/dx=1.3808x-0.0712$
	t=x	35	$y=0.0043x^2+0.0048x+1.2688$	0.9287	$dy/dx=0.0086x+0.0048$
	mV=y	30	$y=-0.125x^2+1.8512x+277.98$	0.3819	$dy/dx=-0.25x+1.8512$
	t=x	35	$y=0.0179x^2-0.1012x+286.63$	0.0085	$dy/dx=0.0358x-0.1012$
Vinegar + phosphoric acid	pH=y	30	$y=-0.0229x^2+0.2002x+1.9993$	0.3178	$dy/dx=-0.0458x+0.2002$
	t=x	35	$y=0.006x^2+0.0098x+2.2138$	0.9439	$dy/dx=0.012x+0.0098$
	mV=y	30	$y=-0.2202x^2+2.0179x+230.66$	0.3929	$dy/dx=-0.4404x+2.0179$
	t=x	35	$y=0.125x^2-1.6607x+236.66$	0.1793	$dy/dx=0.25x-1.6607$
<i>S. cerevisiae</i> + <i>A. aceti</i> + phosphoric acid	pH=y	30	$y=0.0111x^2-0.0401x+2.2832$	0.6787	$dy/dx=-0.0222x-0.0401$
	t=x	35	$y=0.0118x^2-0.022x+2.3736$	0.944	$dy/dx=-0.0236x-0.022$
	mV=y	30	$y=-0.1964x^2+1.0417x+233.7$	0.1235	$dy/dx=0.3928x+1.0417$
	t=x	35	$y=-0.1012x^2-0.8869x+229.7$	0.7201	$dy/dx=-0.2024x-0.8869$

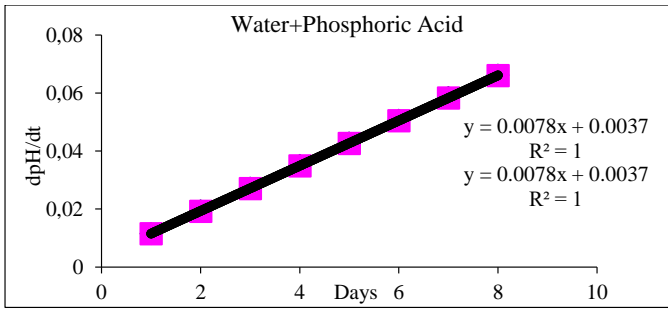


Figure 17. $\frac{dpH}{dt}$ vs t changes for water + phosphoric acid mixture

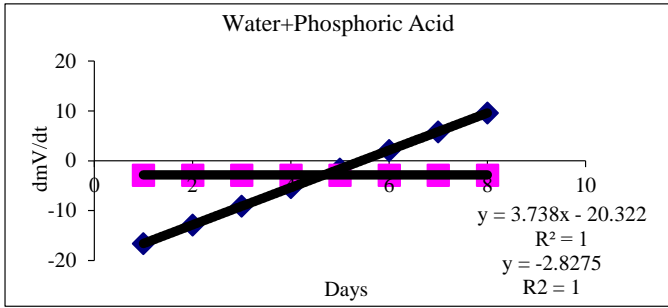


Figure 18. $\frac{dmV}{dt}$ vs t changes for water + phosphoric acid mixture

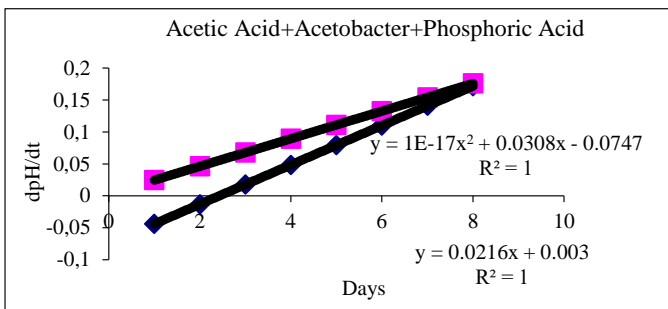


Figure 19. $\frac{dpH}{dt}$ vs t changes for acetic acid + *A. aceti* + phosphoric acid mixture

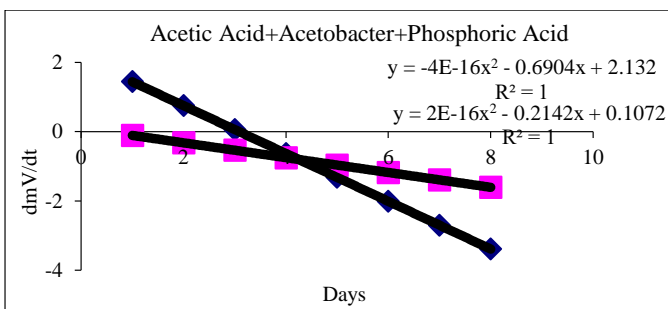


Figure 20. $\frac{dmV}{dt}$ vs t changes for acetic acid + *A. aceti* + phosphoric acid mixture

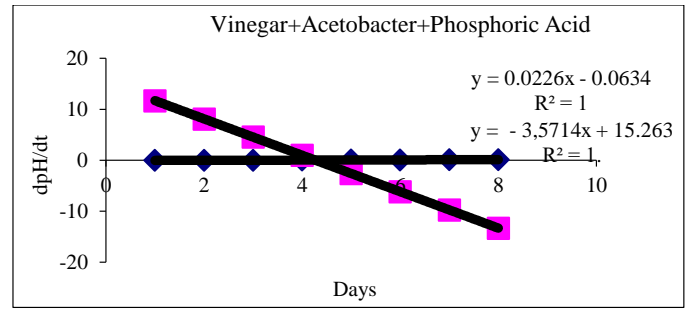


Figure 21. $\frac{dpH}{dt}$ vs t changes for vinegar + *A. aceti* + phosphoric acid mixture

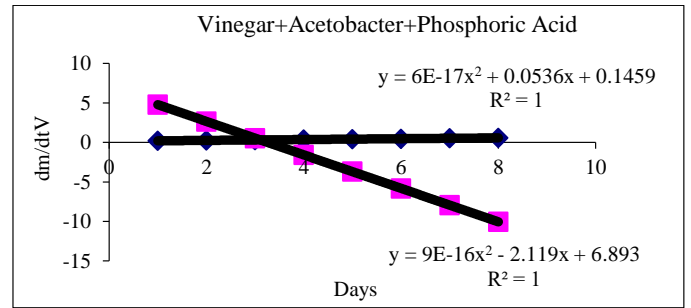


Figure 22. $\frac{dmV}{dt}$ vs t changes for vinegar + *A. aceti* + phosphoric acid mixture

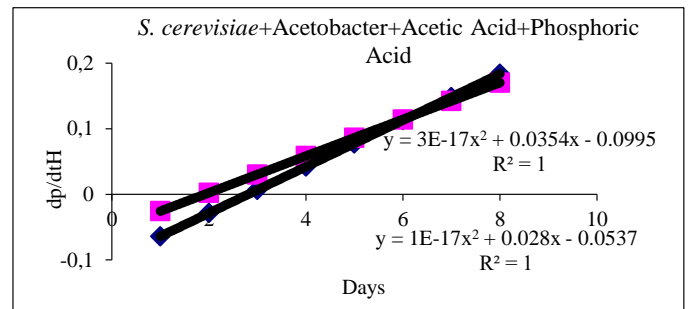


Figure 23. $\frac{dpH}{dt}$ vs t changes for *S. cerevisiae* + *A. aceti* + acetic acid + phosphoric acid mixture

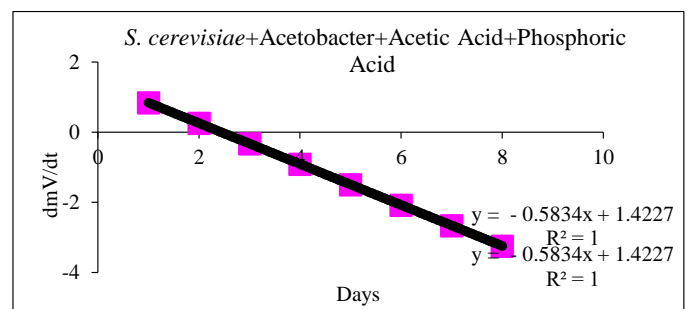


Figure 24. $\frac{dmV}{dt}$ vs t changes for *S. cerevisiae* + *A. aceti* + acetic acid + phosphoric acid mixture

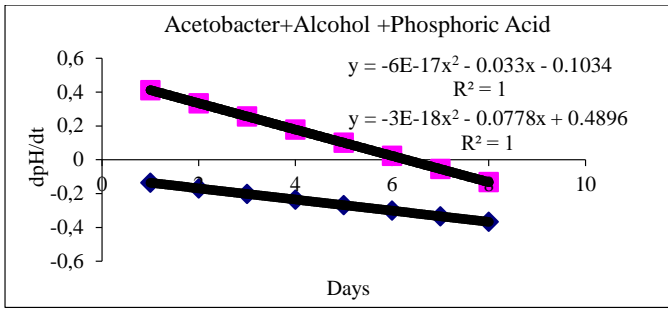


Figure 25. $\frac{dpH}{dt}$ vs t changes for *A. aceti* + alcohol + phosphoric acid mixture

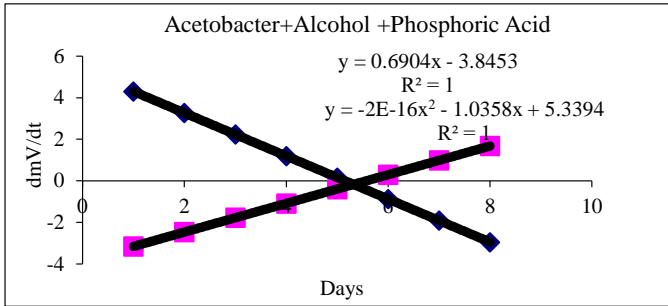


Figure 26. $\frac{dmV}{dt}$ vs t changes for *A. aceti* + alcohol + phosphoric acid mixture

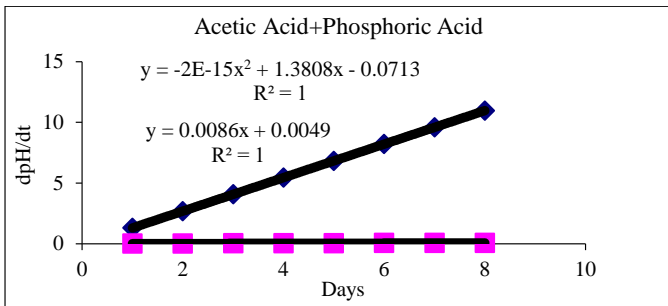


Figure 27. $\frac{dpH}{dt}$ vs t changes for acetic acid + phosphoric acid mixture

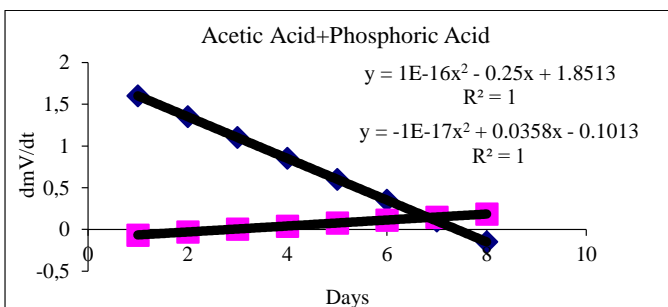


Figure 28. $\frac{dmV}{dt}$ vs t changes for acetic acid + phosphoric acid mixture

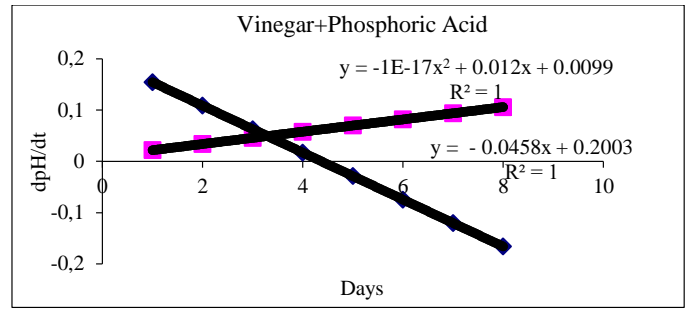


Figure 29. $\frac{dpH}{dt}$ vs t changes for vinegar + phosphoric acid mixture

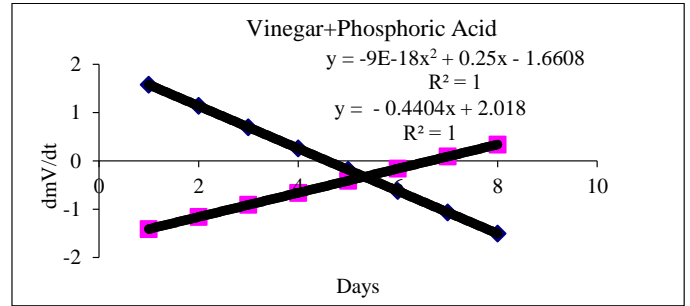


Figure 30. $\frac{dmV}{dt}$ vs t changes for vinegar + phosphoric acid mixture

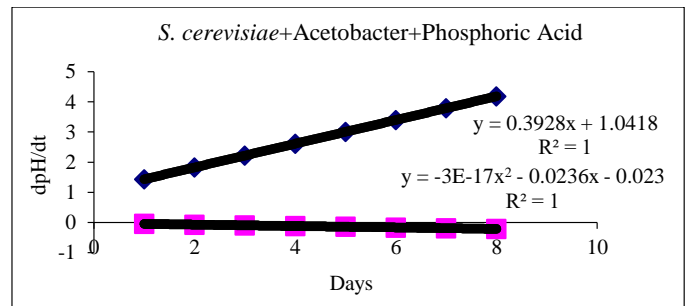


Figure 31. $\frac{dpH}{dt}$ vs t changes for *S. cerevisiae* + *A. aceti* + phosphoric acid mixture

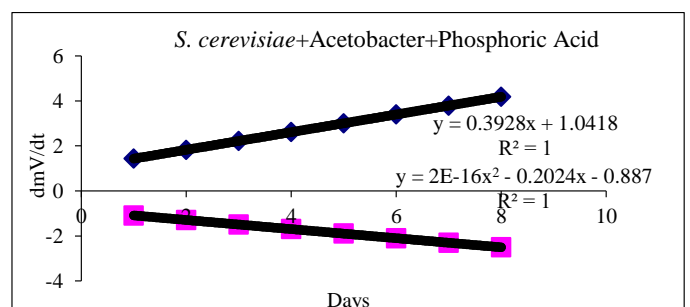
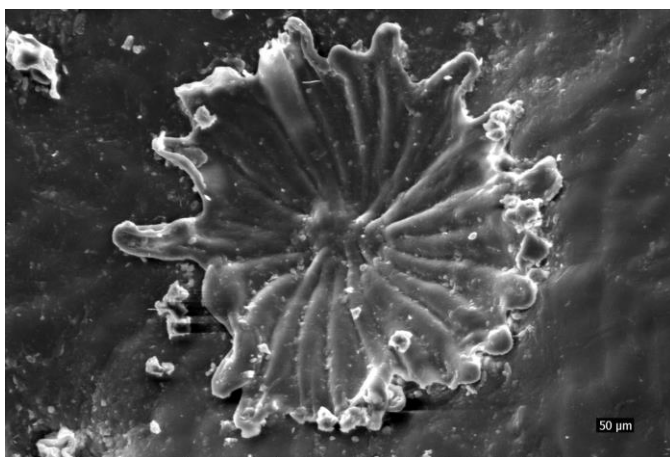


Figure 32. $\frac{dmV}{dt}$ vs t changes for *S. cerevisiae* + *A. aceti* + phosphoric acid mixture

Table 2. Calculated specific kinetic constant values

Pulp solutions		T°C	k (1/time)
Water + phosphoric acid	pH	30	0.007
		35	0.007
	mV	30	0.03
		35	0.03
Acetic acid + <i>A. aceti</i> + phosphoric acid	pH	30	-0.15
		35	-0.55
	mV	30	0.003
		35	0.04
Vinegar + <i>A. aceti</i> + phosphoric acid	pH	30	0.001
		35	-0.1
	mV	30	0.02
		35	0.03
<i>S. cerevisiae</i> + <i>A. aceti</i> + acetic acid + phosphoric acid	pH	30	-0.2
		35	-0.2
	mV	30	0.1
		35	-0.04
<i>A. aceti</i> + alcohol + phosphoric acid	pH	30	0.6
		35	-0.3
	mV	30	0.5
		35	0.001
Acetic acid + phosphoric acid	pH	30	0.2
		35	0.1
	mV	30	0.2
		35	0.1
Vinegar + phosphoric acid	pH	30	0.15
		35	-0.35
	mV	30	0.45
		35	-0.3
<i>S. cerevisiae</i> + <i>A. aceti</i> + phosphoric acid	pH	30	0.4
		35	-0.002
	mV	30	0.3
		35	-0.15

The very highest resolution microstructural imaging of roughly grinded olive tree leaf powder was provided using the Field Emission Scanning Electron Microscopy (FEG-SEM) as much as in the size of 50 μm as shown in Figure 33.

**Figure 33.** FEG-SEM image of the grinded olive leaf powder after the incubation

4. Discussions

Instructive modeling of pH and redox potential changes was investigated showing each modeling step for the determination

of kinetic constants of growth of *A. aceti* and *S. cerevisiae* in variety of combinations of olive leaf, phosphoric acid, acetic acid, ethyl alcohol and vinegar containing incubation media. The incubation experiments in liquid state fermentation process were experimented at lowest pH and different high temperatures of 30 °C and 35 °C for eight days. The detected pH and redox potential values exhibited a steady increase due to the electrochemical, biochemical and biological action responses in bioprocess, and constant microbial growth of *A. aceti* and *S. cerevisiae* was observed during the incubation. The responses of biomolecular mechanisms of *A. aceti* and *S. cerevisiae* microorganisms have shown a persistent microbial growth during the incubation. Acidic solutions effect pH and redox potential values which were regulated by the microbial growth that organisms tend to moderate the pH and redox potential of incubation media. Low pH and redox potential values were obtained with addition of vinegar, acetic acid, phosphoric acid that would have an increasing effect on dissolution of phenolic substances stored in olive tree leaf. The impact of chemicals and biochemicals used for the incubation on *A. aceti* and *S. cerevisiae* organisms is assumed that the activity of the microorganisms almost ceased and the secretion of metabolites increased at the low pH values. At the increased pH values, steady growth of *A. aceti* and *S. cerevisiae* was experimented through the incubation. The metabolic activity of microorganisms was assumed to play the central role in the dissolution, phosphorylation and neutralization process, resulting increase in pH and redox potential as shown in Figures 1 to 16.

The highest kinetic constant estimations were possessed in *A. aceti* + Alcohol + phosphoric acid combination in pH and redox potential values at 30 °C as presented in Table 2. The mixtures of water + phosphoric acid, vinegar + *A. aceti* + phosphoric acid, *S. cerevisiae* + *A. aceti* + acetic acid + phosphoric acid processes at 30 °C, and acetic acid + phosphoric acid and vinegar + phosphoric acid at 35 °C have demonstrated an increase in pH and in redox potential values. *A. aceti* + alcohol + phosphoric acid, vinegar + phosphoric acid, *S. cerevisiae* + *A. aceti* + acetic acid + phosphoric acid solution and *S. cerevisiae* + *A. aceti* + phosphoric acid processes at 30 °C, and vinegar + *A. aceti* + phosphoric acid, *S. cerevisiae* + *A. aceti* + acetic acid + phosphoric acid and *S. cerevisiae* + *A. aceti* + phosphoric acid processes at 35 °C have stated a decrease in pH and in redox potential values as presented in Table 3.

Table 3. The relationship between pH and mV changes in process

Solution mixtures	T°C	pH	mV
Water + phosphoric acid	30	Δ	Δ
	35	Δ	—
Acetic acid + <i>A. aceti</i> + phosphoric acid	30	Δ	▼
	35	Δ	▼
Vinegar + <i>A. aceti</i> + phosphoric acid	30	Δ	Δ
	35	▼	▼
<i>S. cerevisiae</i> + <i>A. aceti</i> + acetic acid + phosphoric acid	30	Δ	Δ
	35	▼	▼
<i>A. aceti</i> + alcohol + phosphoric acid	30	▼	▼
	35	▼	▼
Acetic acid + phosphoric acid	30	▼	Δ
	35	Δ	Δ
Vinegar + phosphoric acid	30	▼	▼
	35	Δ	Δ
<i>S. cerevisiae</i> + <i>A. aceti</i> + phosphoric acid	30	▼	▼
	35	▼	▼

An advanced FEG-SEM technology was used to detect the microstructure image of the pure unprocessed powdered olive tree leaf which was presented as much as in the size of 50 μm as shown in Figure 33. The actual upmost resolution microstructural imaging indicated that the surface of the microparticle of the olive tree leaf possesses high brightness imperfect glazing pores and crisp crack patterns. It's well known that the active compounds of the olive leaf could be extracted in acids and alcohol containing media.

5. Conclusions

It has been shown experimentally that the recorded data of pH and redox potential exhibited a steady increase and demonstrated direct relationship between pH and the redox potentials in this chemical, biochemical and biological processes, that a constant microbial growth was observed at lowest pH and high temperatures. Increase in pH value displayed increase in redox potential in water + phosphoric acid, vinegar + A. *aceti* + phosphoric acid, S. *cerevisiae* + A. *aceti* + acetic acid + phosphoric acid, and S. *cerevisiae* + A. *aceti* + phosphoric acid processes at 30 °C and acetic acid + phosphoric acid and vinegar + phosphoric acid processes at 30 °C. Decrease in pH value displays decrease in redox potential in A. *aceti* + alcohol + phosphoric acid, vinegar + phosphoric acid, S. *cerevisiae* + A. *aceti* + acetic acid + phosphoric acid, and S. *cerevisiae* + A. *aceti* + phosphoric acid processes at 30 °C and vinegar + A. *aceti* + phosphoric acid, S. *cerevisiae* + A. *aceti* + acetic acid + phosphoric acid, and S. *cerevisiae* + A. *aceti* + phosphoric acid processes at 35 °C.

References

- Borjan, D., Leitgeb, M., Knez, Ž. & Hrnčič, M. K. (2020). Microbiological and antioxidant activity of phenolic compounds in olive leaf extract. *Molecules*, 25(24), 5946. doi:10.3390/molecules25245946
- Chen, C. G., Nardi, A. N., Amadei, A. & D'Abramo, M. (2022). Theoretical modeling of redox potentials of biomolecules. *Molecules*, 27, 1077. doi:10.3390/molecules27031077
- Ermurat, Y. (2013). Modeling the kinetics of pyrite ash biodesulfurization by *Saccharomyces cerevisiae* and *Acetobacter aceti* in liquid state bioreactors. *Electronic Journal of Biotechnology*, 16(2), 4-4. doi:10.2225/vol16-issue2-fulltext-1.
- Krisch, J. & Szajani, B. (1996). Effects of immobilization on biomass production and acetic acid fermentation of *Acetobacter aceti* as a function of temperature and pH. *Biotechnology Letters*, 18, 393-396. doi:10.1007/BF00143458
- Krisch, J. & Szajani, B. (1997). Ethanol and acetic acid tolerance in free and immobilized cells of *Saccharomyces cerevisiae* and A. *aceti*. *Biotechnology Letters*, 19, 525-528. doi:10.1023/A:1018329118396
- Markhali, F. S., Teixeira, J. A. & Rocha, C. M. R. (2020). Olive tree leaves—a source of valuable active compounds. *Processes*, 8, 1177. doi:10.3390/pr8091177
- Neuer, B., Plagens, U. & Werner, D. (1983). Phosphodiester bonds between polypeptides and chromosomal DNA. *Journal of Molecular Biology*, 164, 213-235. doi:10.1016/0022-2836(83)90076-1
- Ory, I., Romero, L. & Cantero, D. (1998). Modelling the kinetics of growth of *Acetobacter aceti* in discontinuous culture: influence of the temperature of operation. *Applied Microbiology and Biotechnology*, 49, 189-193. doi:10.1007/s002530051157
- O'Sullivan, J. & Ettlinger, L. (1976). Characterization of the acetyl-CoA synthetase of *Acetobacter aceti*. *Biochimica et Biophysica Acta BBA-Lipids and Lipid Metabolism*. 450, 410-417. doi:10.1016/0005-2760(76)90014-X
- Qabaha, K., AL-Rimawi, F., Qasem, A. & Naser, S. A. (2018). Oleuropein is responsible for the major anti-inflammatory effects of olive leaf extract. *Journal of Medicinal Food*, 302-305. doi:10.1089/jmf.2017.0070
- Radak, B. K., Chipot, C., Suh, D., Jo, S., Jiang, W., Phillips, J. C., Schulten, K. & Roux, B. (2017). Constant-pH molecular dynamics simulations for large biomolecular systems. *Journal of Chemical Theory and*

Computation, 1312, 5933-5944. doi:10.1021/acs.jctc.7b00875

Tarrant, M. K. & Cole, P. A. (2009). The chemical biology of protein phosphorylation. *Annual Review of Biochemistry*, 78, 797-825. doi:10.1146/annurev.biochem.78.070907.103047

Topuz, S. & Bayram, M. (2021). Oleuropein extraction from leaves of three olive varieties (*Olea europaea L.*): Antioxidant and antimicrobial properties of purified oleuropein and oleuropein extracts. *Journal of Food Processing and Preservation*, e15697 doi:10.1111/jfpp.15697